HTML ABSTRACT + LINKS

Bias conditions of dc-SQUID for a time-domain SQUID multiplexer

Jörn Beyer[a] and Dietmar Drung
Physikalisch-Technische Bundesanstalt Berlin, Abbestrasse 2-12, 10587 Berlin, Germany

Kent D. Irwin
National Institute of Standards and Technology, Mail Stop 814.03, 325 Broadway, Boulder, Colorado 80303

(Received 4 August 2003; accepted 6 November 2003)

We have analyzed the biasing of the first-stage dc superconducting quantum interference devices (SQUIDs) of a time-domain dc-SQUID multiplexer (SQUID MUX) and find that the bias conditions of first-stage SQUIDs significantly affect the performance of the SQUID MUX in terms of total multiplexer noise and bandwidth. We present an experimental study of the operational parameters of a first-stage SQUID under varied bias conditions. Our measurements include a direct determination of the first-stage SQUID dynamic resistance R_{DYN1} and the flux noise of the first-stage SQUID biased over the range from voltage bias to current bias. Our measurements show that matching the bias resistors R_{S1} of the first-stage SQUIDs to R_{DYN1} improves the SQUID MUX noise performance as well as the first-stage bandwidth. © *2004 American Institute of Physics.*
[DOI: 10.1063/1.1638877]

I. INTRODUCTION

Superconducting quantum interference devices (SQUIDs) are commonly used as current amplifiers to read out low-impedance cryogenic detectors.[1–3] In these circuits, several stages of dc-SQUIDs can be used. The cryogenic detector is usually read out by a voltage-biased dc-SQUID which in turn is coupled to a current-biased dc-SQUID or dc-SQUID series array.[2] The same concept has been applied to a time-domain dc-SQUID multiplexer (SQUID MUX) for the read-out of large-scale arrays of cryogenic detectors.[4] Such arrays of cryogenic detectors are under development for a variety of applications ranging from sub-millimeter astronomy[5] to x-ray spectroscopy.[6]

The basic scheme of one column of this SQUID MUX is depicted in Fig. 1(a). The output of each detector couples magnetic flux into an individual first-stage SQUID denoted as SQ1. Multiplexing between different detectors in one column is performed by switching the bias of the corresponding SQ1 on and off. The second-stage SQUID SQ2 is constantly biased and acts as a low-noise cryogenic current amplifier for the column. In order to read out two-dimensional detector arrays a number of SQUID MUX columns are combined.

The most important aspects of the operating performance of a SQUID multiplexer are the system noise, the bandwidth, and the power dissipated. The bias conditions of the first-stage SQUIDs affect these parameters significantly.

II. THEORY

Usually, dc-SQUIDs are denoted as ''current biased'' when the average current I_{SQ} through the SQUID remains constant, or ''voltage biased'' when the average voltage V_{SQ} across the SQUID is kept constant. For ideal voltage bias, I_{SQ} changes in response to a magnetic flux Φ_{SQ} with a transfer coefficient $I_\Phi = \partial I_{\mathrm{SQ}}/\partial \Phi_{\mathrm{SQ}}$, whereas for ideal current bias, V_{SQ} changes and the transfer coefficient is $V_\Phi = \partial V_{\mathrm{SQ}}/\partial \Phi_{\mathrm{SQ}}$. In both bias modes, the relevant transfer coefficient, I_Φ or V_Φ, depends strongly on the actual bias conditions.

The SQUID bias is achieved in practice by applying a current I_{BIAS} to the SQUID shunted by a resistor R_S. Near-ideal current or voltage bias is, therefore, operant when R_S is much greater or smaller than the SQUID dynamic or differential resistance $R_{\mathrm{DYN}} = \partial V_{\mathrm{SQ}}/\partial I_{\mathrm{SQ}}$. Note that R_{DYN} is generally greater than both the equivalent resistance $R_{\mathrm{SQ}} = V_{\mathrm{SQ}}/I_{\mathrm{SQ}}$ of the biased SQUID and the asymptotic normal-state resistance R_N of the SQUID. Deviations from the conditions $R_S \ll R_{\mathrm{DYN}}$ for voltage bias and $R_S \gg R_{\mathrm{DYN}}$ for current bias ''soften'' the respective bias mode. In this case, the small-signal behavior of the SQUID may be described by the total differential[7]

$$dV_{\mathrm{SQ}} = V_\Phi d\Phi + R_{\mathrm{DYN}} dI_{\mathrm{SQ}}. \tag{1}$$

Setting $dV_{\mathrm{SQ}} = 0$ yields the relation $I_\Phi = -V_\Phi/R_{\mathrm{DYN}} = -1/M_{\mathrm{DYN}}$ between the intrinsic or unloaded transfer coefficients I_Φ and V_Φ for ideal voltage and current bias and the SQUID dynamic resistance. Here, M_{DYN} denotes the current sensitivity of the unloaded SQUID.[7]

In a two-stage SQUID configuration with the first-stage SQUID no longer under near-ideal voltage bias, the current through the second-stage input coil L_{IN2} can still be considered the output current of SQ1. However, the loaded flux-to-current transfer coefficient of SQ1 (shunted by R_{S1}) becomes

$$I_{\Phi 1} = -V_{\Phi 1}/(R_{\mathrm{DYN1}} + R_{S1}). \tag{2}$$

Note, that here $V_{\Phi 1}$ is still the intrinsic SQ1 flux-to-voltage transfer coefficient.

It is clear from Fig. 1(a) that the Johnson noise of *all* resistors R_{S1} in a multiplexed column contribute to the noise

[a]Author to whom correspondence should be addressed; electronic mail: joern.beyer@ptb.de

 © 2004 American Institute of Physics

Downloaded 04 Feb 2010 to 132.163.130.14. Redistribution subject to AIP license or copyright; see http://rsi.aip.org/rsi/copyright.jsp

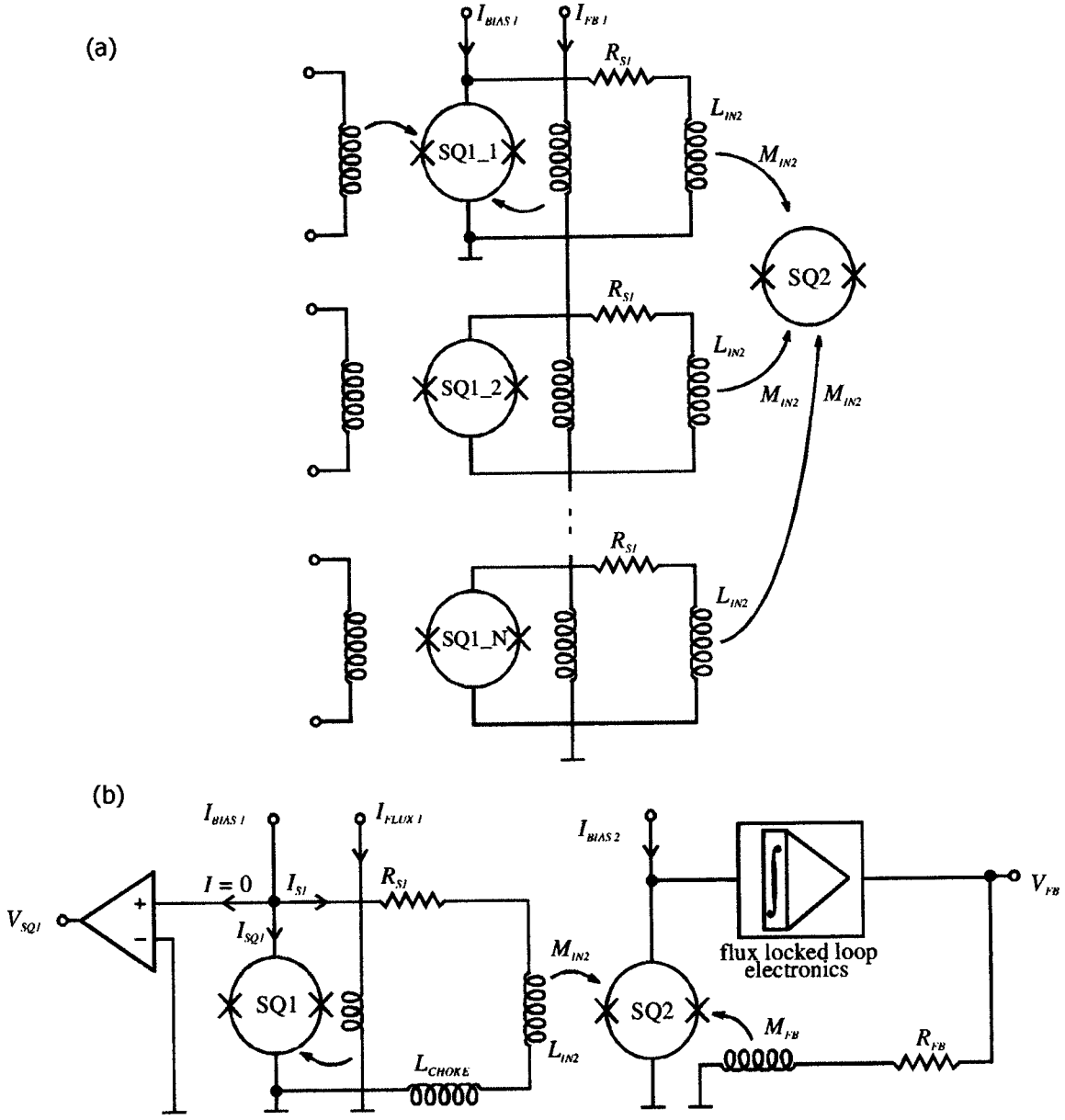

FIG. 1. (a) Basic scheme of an N channel column of a time-domain SQUID multiplexer, and (b) the setup used to measure the operating parameters of a first-stage SQUID SQ1 under varied bias conditions.

of a biased SQUID MUX channel. For the scheme depicted in Fig. 1(a) the total noise of the SQUID MUX column can be expressed as the flux noise $S_{\Phi 1}$ of the particular channel that is switched on:

$$S_{\Phi 1} = S_{\Phi i1} + 4k_B \mathrm{T} R_{S1}/V_{\Phi 1}^2 + (N-1)4k_B T(R_{\mathrm{DYN1}} + R_{S1})^2/V_{\Phi 1}^2 R_{S1} + (S_{\Phi 2}/M_{\mathrm{IN2}}^2)(R_{\mathrm{DYN1}} + R_{S1})^2/V_{\Phi 1}^2, \quad (3)$$

where $S_{\Phi 2}$ is the SQ2 flux noise, M_{IN2} is the SQ2 input mutual inductance, k_B is the Boltzmann constant, and T is the first-stage temperature. Besides the SQ1 intrinsic flux noise $S_{\Phi i1}$, the terms on the right in Eq. (2) represent the noise contribution of the R_{S1} of the biased SQ1, the Johnson noise of the shunt resistors of the unbiased channels, and the flux noise of SQ2 related to the biased SQ1. For transparency, we subsume noise contributions of amplifier stages following SQ2 in the current noise of the second stage ($S_{\Phi 2}/M_{\mathrm{IN2}}^2$). Furthermore, parasitic noise sources, such as damping resistors, are not considered here.

From Eq. (3) it can be seen that there is a particular value of R_{S1} at which the Johnson noise contribution of the shunt resistors is minimum. If the last term in Eq. (3) can be neglected, i.e., if SQ2 and the following stages of the amplifier chain do not contribute significantly to the system noise, this optimum value is easily found to be

$$R_{S1} = R_{\mathrm{DYN1}} \sqrt{(1 - 1/N)}. \quad (4)$$

Equation (4) suggests that—assuming $S_{\Phi i1}$ and R_{DYN1} are unaffected by the bias conditions—for N on the order of 10–100 the bias of the first-stage SQUIDs should be between voltage and current bias in order to achieve optimum noise performance of the SQUID MUX. An increased value of R_{S1} is also preferable in two other respects. First, the power P

Downloaded 04 Feb 2010 to 132.163.130.14. Redistribution subject to AIP license or copyright; see http://rsi.aip.org/rsi/copyright.jsp

$\approx V_{SQ1}I_{SQ1}+V_{SQ1}^2/R_{S1}$ dissipated when biasing SQ1 is reduced with an increased R_{S1}. Second, the bandwidth of the low-pass filter formed by SQ1, R_{S1}, and the SQ2 input inductance L_{IN2} is increased. The characteristic frequency of that low-pass filter is

$$f_{3dB}=(R_{DYN1}+R_{S1})/2\pi(L_{IN2}+L_{STRAY}). \quad (5)$$

Here, L_{STRAY} includes any parasitic inductances in the first-stage circuit. The first-stage bandwidth is an important design criterion, as it can be a dominant pole in the overall transfer function and, hence, limit the SQUID MUX sampling speed.[8]

III. EXPERIMENTS

We experimentally investigated the effect of different SQUID bias conditions in a two-stage configuration depicted in Fig. 1(b). The first-stage SQUID under investigation was a dc SQUID of rectangular washer design with a loop inductance $L_{SQ1}\approx 15\,\mathrm{pH}$, a total critical current $I_C\approx 100\,\mu\mathrm{A}$, and a SQUID normal-state resistance $R_N\approx 0.7\,\Omega$. It was fabricated with a $Nb/Al_2O_3/Nb$ process on silicon.[9] The SQUID leads were connected symmetrically to the washer so that the bias current in these leads does not inductively couple to the SQUID. A single-turn coil around the washer was used to "flux-bias," i.e., to apply a certain magnetic flux Φ_{SQ1} to SQ1. We used a 30-SQUID series array[10] as the low-noise second-stage amplifier. The experiments were performed with both SQ1 and SQ2 inside a superconducting magnetic shield in liquid helium at 4.2 K.

Our measurement setup differs from the two-stage SQUID configuration in Ref. 2. First, we operated the second-stage SQUID in a flux-locked loop (FLL). Second, we inserted a choke inductor—a Cu wire wound coil—with $L_{CHOKE}\gg L_{IN2}+L_{STRAY}$ into the circuit that couples the output of SQ1 to the SQ2 input. Hence, Eq. (5) becomes

$$f_{3dB}=(R_{DYN1}+R_{S1}+R_{CHOKE})/2\pi(L_{CHOKE}+L^*_{IN2}+L_{STRAY}). \quad (6)$$

Here, L^*_{IN2} is the SQ2 input inductance in FLL operation which differs from L_{IN2} due to the magnetic coupling between feedback and input coils. R_{CHOKE} is the parasitic resistance of the choke inductor in the first-stage circuit. From the value of f_{3dB} the SQ1 dynamic resistance R_{DYN1} can be determined. In this way R_{DYN1} can be measured directly under the exact conditions of SQ1 operation without taking the $I_{SQ1}-V_{SQ1}$ curve.[11] In order to determine R_{DYN1} from f_{3dB} as accurately as possible, it is advisable to choose the inductance L_{CHOKE} such that the pole of the input circuit differs significantly from other poles in the transfer function of the two-stage configuration. We also measured the dc voltage V_{SQ1} across SQ1 directly. This is necessary to determine the current I_{SQ1} through SQ1 by subtracting the current $I_{S1}=V_{SQ1}/(R_{S1}+R_{CHOKE})$ from the total bias current I_{BIAS1}.

Our measurement procedure was as follows. The second-stage SQUID array was operated in FLL with a bandwidth of about 0.85 MHz. With SQ1 *unbiased*, the flux noise spectrum of the SQUID array was taken. The Johnson noise of the first-stage shunt resistor R_{S1} causes a distinct excess flux noise $S_X=4k_BTM_{IN2}/(R_{S1}+R_{CHOKE})$ which shows a first-order low-pass response with the corner frequency $f_{3dB}=f_X$ obtained from Eq. (6) for $R_{DYN1}=0$. The excess noise spectrum, therefore, gives a measure of $(R_{S1}+R_{CHOKE})$ and $L_{TOTAL}=L_{CHOKE}+L^*_{IN2}+L_{STRAY}$. Figure 2(a) shows such a SQ2 flux noise spectrum. From the corresponding fitting curves for the SQ2 total flux noise $S_{TOTAL2}=S_X/(1+f^2/f_X^2)+S_{\Phi 2}$ we extracted the values $R_{S1}+R_{CHOKE}=0.96$, 3.4, and 9.6 Ω for the three different shunt resistors used. Furthermore, the values for the total first-stage inductance $L_{TOTAL}=20.5\,\mu\mathrm{H}$, and the second-stage flux noise $S_{\Phi 2}=0.19\,\mu\Phi_0/\sqrt{\mathrm{Hz}}$ were obtained from these fitting curves. The parasitic resistance of the choke inductor has

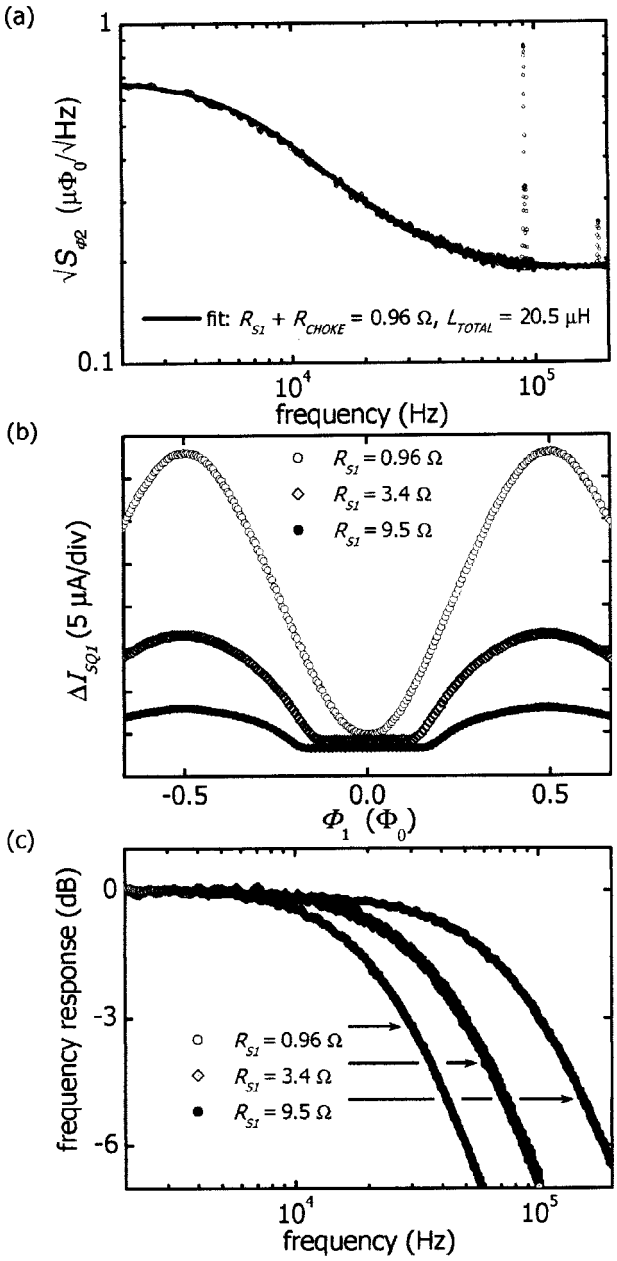

FIG. 2. (a) Flux noise spectrum of SQ2 for unbiased SQ1 with shunt resistor $R_{S1}+R_{CHOKE}=0.96\,\Omega$ and corresponding fitted curve, (b) apparent current-flux characteristics, and (c) normalized frequency response of SQ1 for the different R_{S1}. In (c) the first-stage SQUID was flux-biased for minimum flux noise $S_{\Phi 1}$. Curves in (b) are vertically shifted for clarity.

Downloaded 04 Feb 2010 to 132.163.130.14. Redistribution subject to AIP license or copyright; see http://rsi.aip.org/rsi/copyright.jsp

been measured independently to be $R_{\mathrm{CHOKE}} \approx 15\,\mathrm{m}\Omega$.

The performance of the biased SQ1 was investigated with SQ2 kept in FLL operation. The measurements taken involve the flux transfer from SQ1 to SQ2 and the flux noise of SQ1. To enable the measurement results obtained for different shunt resistors to be compared, the applied currents I_{BIAS1} were adjusted so that the current through the first-stage SQUID without bias flux applied to SQ1, $I_{\mathrm{SQ1}} = I_{\mathrm{BIAS1}} - V_{\mathrm{SQ1}}/(R_{S1} + R_{\mathrm{CHOKE}})$, was the same for each data set.

In Fig. 2(b) the loaded SQ1 current-flux characteristics for $I_{\mathrm{SQ1}} = 121\ \mu\mathrm{A}$ and the three different R_{S1} are shown. The curves were obtained by applying a low-frequency magnetic flux to SQ1 and monitoring the flux coupled into SQ2 via L_{IN2}. In the same way, the loaded transfer coefficient $I_{\Phi 1}$ has been measured but with a reduced magnetic flux signal of about $0.015\,\Phi_0$ in SQ1. Since in our measurement setup the FLL is operated with respect to SQ2, the transfer coefficient $I_{\Phi 1}$ is needed to determine the first-stage flux noise from the current noise coupled into SQ2 via L_{IN2}.

To obtain the frequency response curves in Fig. 2(c), random white noise corresponding to $\approx 1\ \mu\Phi_0/\sqrt{\mathrm{Hz}}$ and a frequency range extending well beyond $f_{3\mathrm{dB}}$ was applied to SQ1. In analogy to the $R_{S1} + R_{\mathrm{CHOKE}}$ and L_{TOTAL} measurements, we numerically fitted these frequency response curves with the transfer function of a first-order low-pass response to obtain $f_{3\mathrm{dB}}$ from which we can calculate R_{DYN1}.

We performed measurements of the loaded flux-to-current transfer coefficient, the flux noise, and the dynamic resistance of SQ1 on the positive branch of the symmetric first-stage current-flux characteristics shown in Fig. 2(b). The results are plotted in Fig. 3 together with the part of the current-flux characteristics on which the working points were chosen. The SQ1 flux noise represents the actual flux noise of the first stage, i.e., we subtracted $S_{\Phi 2}$. We find that for all three shunt resistor values the minimum SQ1 flux noise is measured for a flux bias at which the transfer coefficient $I_{\Phi 1}$ is maximum. However, the flux bias range for minimum SQ1 flux noise becomes narrower with increased R_{S1}. We can compare the measured flux noise with the values expected theoretically, i.e., with the sum of the first two terms on the right in Eq. (3). If we use the relation $S_{\Phi i1} = 9 k_B T L_{\mathrm{SQ1}}^2 / R_N$ for the SQ1 intrinsic flux noise[12,13] we find that the measured first-stage flux noise for all three shunt resistor values is only 10%–15% higher than in theory. In Fig. 3(d) the dynamic resistances R_{DYN1} determined from the $f_{3\mathrm{dB}}$ in Eq. (6) are shown. The error bars display the uncertainty in the fitting parameters. It can be seen that for working points well on the flank of the current-flux characteristics, the R_{DYN1} values do not significantly differ for the three different shunt resistor values. This result is reasonable as for the same current I_{SQ1} and the same applied magnetic flux Φ_{SQ1} the first-stage SQUID should be at the same point on the $I_{\mathrm{SQ1}} - V_{\mathrm{SQ1}}$ curve. In the flux bias range for minimum SQ1 flux noise we find R_{DYN1} values of 3.1–3.8 Ω. As expected, the intrinsic transfer coefficients $V_{\Phi 1}$ calculated with Eq. (2) for the relevant working points are also not strongly affected by the different shunt resistor values.

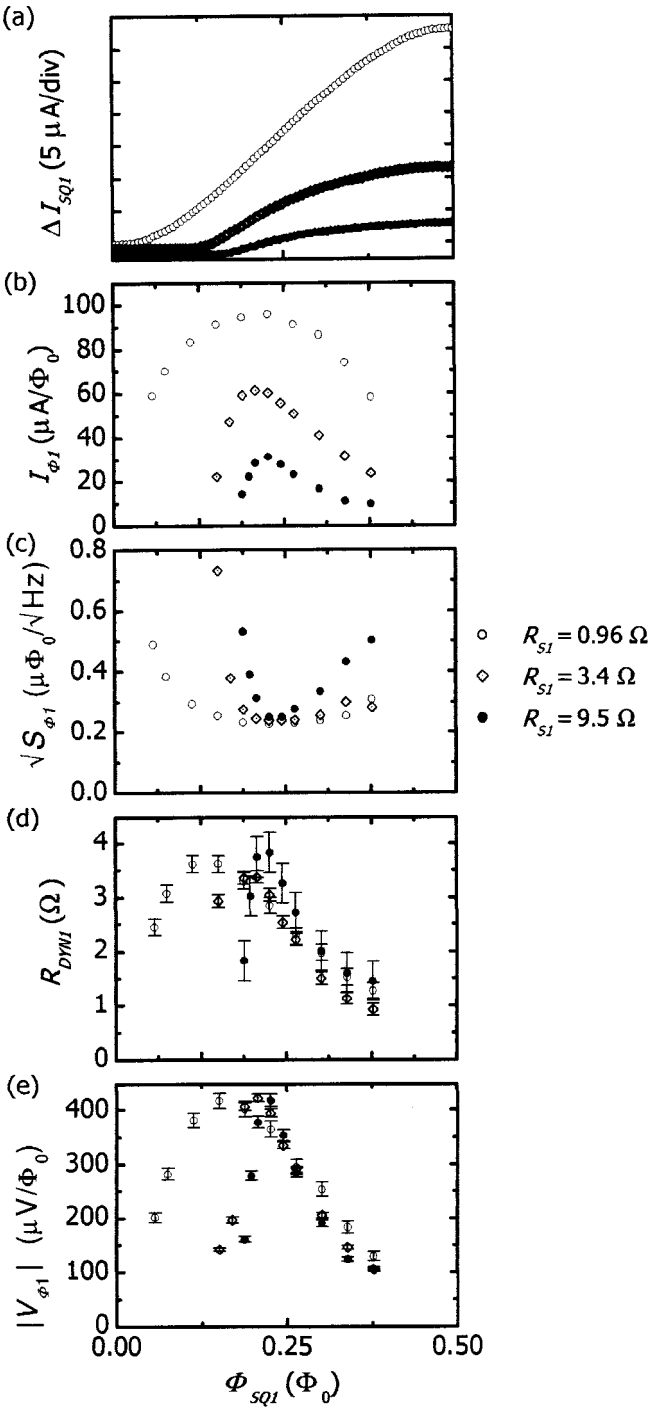

FIG. 3. SQ1 parameters $I_{\Phi 1}$, $S_{\Phi 1}$, R_{DYN1}, and $V_{\Phi 1}$ for the three shunt resistors R_{S1} measured at different working points on the current-flux characteristics. (a) Parts of the current-flux curve on which the working points were chosen. The flux axes are the same for all diagrams.

IV. DISCUSSION

For the practical optimization of the time-domain SQUID MUX the measurement results indicate that the first-stage SQUID can be biased in softened voltage bias without significant degradation of the flux noise of the first stage. Based upon our measurement results we estimated the total flux noise $S_{\Phi 1}$ of one out of N SQUID MUX channels according to Eq. (3) for a first-stage operating temperature $T = 0.1\,\mathrm{K}$. Here, we used the minimum SQ1 flux noise mea-

Downloaded 04 Feb 2010 to 132.163.130.14. Redistribution subject to AIP license or copyright; see http://rsi.aip.org/rsi/copyright.jsp

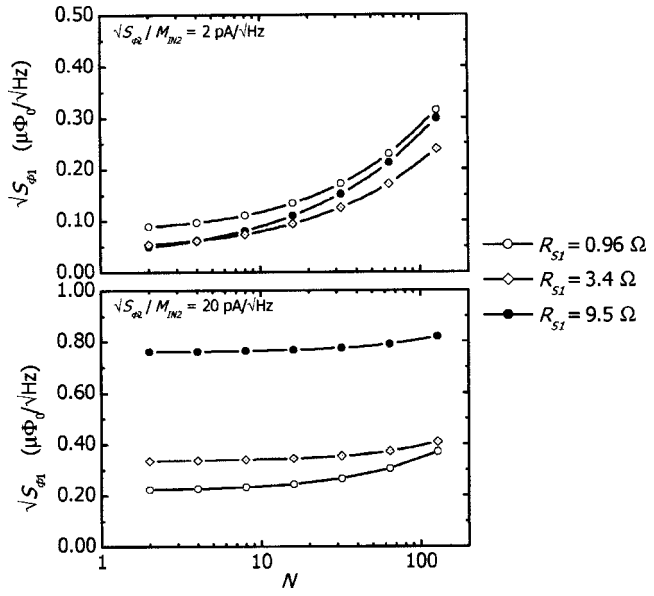

FIG. 4. Flux noise of one channel of an N SQUID MUX estimated using Eq. (3). The minimum measured SQ1 flux noise values for the three shunt resistors R_{S1}, a first-stage operating temperature $T=0.1\,\mathrm{K}$, and $\sqrt{S_{\Phi 2}}/M_{\mathrm{IN2}}=2\,\mathrm{pA}/\sqrt{\mathrm{Hz}}$ and $20\,\mathrm{pA}/\sqrt{\mathrm{Hz}}$ are used.

sured for the respective R_{S1} and the corresponding R_{DYN1} and $V_{\Phi 1}$ values and assumed a temperature dependence of the SQ1 flux noise $\propto\sqrt{T}$. For the second-stage noise contribution values of $\sqrt{S_{\Phi 2}}/M_{\mathrm{IN2}}=2\,\mathrm{pA}/\sqrt{\mathrm{Hz}}$ and $\sqrt{S_{\Phi 2}}/M_{\mathrm{IN2}}=20\,\mathrm{pA}/\sqrt{\mathrm{Hz}}$ were used. The larger value represents the second stage noise contribution for the SQUID MUX configuration discussed in Ref. 8. There, the common superconducting transformer used to couple the first-stage outputs to the second-stage input introduced a comparably low flux coupling to SQ2. A direct coupling of the individual first-stage SQUIDs to SQ2 as depicted in Fig. 1(a) increases the flux coupling to SQ2 and, hence, would reduce the second-stage noise contribution.

In Fig. 4, for $T=0.1\,\mathrm{K}$ and $\sqrt{S_{\Phi 2}}/M_{\mathrm{IN2}}=2\,\mathrm{pA}/\sqrt{\mathrm{Hz}}$, we obtain the minimum SQ1 flux noise for $R_{S1}=3.4\,\Omega$. For $N\geqslant 32$ the noise reduction is about 30% compared to the calculated noise values for $R_{S1}=0.96\,\Omega$ and $R_{S1}=9.5\,\Omega$. This result illustrates the matching condition of Eq. (4) for $\sqrt{S_{\Phi 2}}/M_{\mathrm{IN2}}\rightarrow 0$. This situation changes if the second-stage noise contribution is significant, $\sqrt{S_{\Phi 2}}/M_{\mathrm{IN2}}=20\,\mathrm{pA}/\sqrt{\mathrm{Hz}}$ in our example. Here, an improvement in noise performance with matched bias $R_{S1}\approx R_{\mathrm{DYN1}}$ can only be expected for SQUID MUX channels $N>100$.

In addition to the reduction of the SQUID MUX noise, the increase in the first-stage bandwidth is an important benefit when operating the SQ1 with a matched bias. If this bandwidth is the dominant design criterion, R_{S1} might be increased beyond the matching condition given in Eq. (4). This case is illustrated by the noise estimation for $R_{S1}=9.5\,\Omega$. The increase in the first-stage flux noise for $\sqrt{S_{\Phi 2}}/M_{\mathrm{IN2}}=2\,\mathrm{pA}/\sqrt{\mathrm{Hz}}$ when R_{S1} is increased from 1 to 9.5 Ω is moderate, about 15% for $N\geqslant 32$. This might be acceptable as the first-stage bandwidth is increased by almost a factor of 3.

The analysis and experiments presented were aimed at optimizing the operating performance of a time-domain SQUID multiplexer. Considering the different noise contributions of the SQUID MUX, we find that optimum noise performance of the first-stage SQUID is achieved for a matched SQ1 bias with $R_{S1}\approx R_{\mathrm{DYN1}}$ instead of a near-ideal voltage bias as would be preferable in a single-channel two-stage SQUID configuration. We investigated the operating parameters of a low-noise first-stage SQUID under varied bias conditions. Provided that the current and the flux applied to the SQ1 are the same, the measured minimum flux noise as well as the dynamic resistance were not significantly affected by the different shunt resistors used. Important practical benefits of a matched SQ1 bias are the increased bandwidth and the reduced power dissipation of the first stage. Further increase in bandwidth is possible for $R_{S1}>R_{\mathrm{DYN1}}$ at the cost of degraded SQUID MUX noise performance.

ACKNOWLEDGMENT

Part of the work done by K.D.I. was a contribution of the U.S. Government.

[1] W. Seidel, G. Forster, W. Christen, F. von Feilitzsch, H. Göbel, F. Pröbst, and R. L. Mößbauer, Phys. Lett. B **236**, 483 (1990).
[2] K. D. Irwin, G. C. Hilton, J. M. Martinis, S. Deiker, N. Bergren, S. W. Nam, D. A. Rudman, and D. A. Wollman, Nucl. Instrum. Methods Phys. Res. A **444**, 184 (2000).
[3] A. Fleischmann, T. Daniyarov, H. Rotzinger, M. Link, C. Enss, and G. M. Seidel, Rev. Sci. Instrum. **74**, 3947 (2003).
[4] K. D. Irwin *et al.*, AIP Conf. Proc. **605**, 301 (2002).
[5] W. D. Duncan *et al.*, AIP Conf. Proc. **605**, 577 (2002).
[6] D. A. Wollman, K. D. Irwin, G. C. Hilton, L. L. Dulcie, D. E. Newbury, and J. M. Martinis, J. Microsc. **188**, 197 (1997).
[7] D. Drung and M. Mück, in *SQUID Handbook*, edited by J. Clarke and A. Braginsky (Wiley-VCH, Berlin, 2004), Chap. 4.
[8] P. A. J. de Korte, J. Beyer, S. Deiker, G. C. Hilton, K. D. Irwin, M. MacIntosh, S. W. Nam, C. D. Reintsema, and L. R. Vale, Rev. Sci. Instrum. **74**, 3807 (2003).
[9] J. E. Sauvageau, C. J. Burroughs, P. A. A. Booi, M. W. Cromar, S. P. Benz, and J. A. Koch, IEEE Trans. Appl. Supercond. **5**, 2303 (1995).
[10] R. P. Welty and J. M. Martinis, IEEE Trans. Magn. **27**, 2924 (1991).
[11] V. Polushkin, D. Glowacka, R. Hart, and J. M. Lumley, J. Low Temp. Phys. **118**, 105 (2000).
[12] C. Tesche and J. Clarke, J. Low Temp. Phys. **29**, 301 (1977).
[13] J. J. P. Bruines, V. J. de Waal, and J. E. Mooij, J. Low Temp. Phys. **46**, 383 (1982).

Downloaded 04 Feb 2010 to 132.163.130.14. Redistribution subject to AIP license or copyright; see http://rsi.aip.org/rsi/copyright.jsp